

# A Novel Uplink Multiple Access Scheme Based on TDS-FDMA

Linglong Dai, Zhaocheng Wang, *Senior Member, IEEE*, and Sheng Chen, *Fellow, IEEE*

**Abstract**—This contribution proposes a novel time-domain synchronous frequency division multiple access (TDS-FDMA) scheme to support multi-user uplink application. A unified frame structure for both single-carrier and multi-carrier transmissions and the corresponding low-complexity receiver design are derived. Compared with standard cyclic prefix based orthogonal frequency division multiple access systems, the proposed TDS-FDMA scheme improves the spectral efficiency by about 5% to 10% as well as imposes a similarly low computational complexity, while obtaining a slightly better bit error rate performance over Rayleigh fading channels.

**Index Terms**—Frequency division multiple access, multi-user uplink, orthogonal frequency division multiple access.

## I. INTRODUCTION

**B**Y utilizing pseudorandom noise (PN) sequence instead of cyclic prefix (CP) as the guard interval of the inverse discrete Fourier transform (IDFT) block, time-domain synchronous (TDS) orthogonal frequency division multiplexing (OFDM) outperforms CP based OFDM in spectral efficiency at the cost of a higher complexity. Higher spectral efficiency is achieved without the frequency-domain (FD) pilot insertions. However, the cyclicity of the received IDFT block is destroyed due to the inter-symbol interference (ISI) between the PN sequence and the IDFT block. Therefore, iterative interference cancellation (IC) has to be employed for removing the ISI, in order to achieve more accurate channel estimation (CE) as well as to reconstruct the cyclicity of the received IDFT block for channel equalization [1]. This iterative IC imposes high complexity and may suffer from unsatisfactory performance due to the fact that CE and IC are mutually conditional, namely, perfect CE is needed for ideal IC while perfect IC is required for ideal CE. Nevertheless, TDS-OFDM was adopted as the key technology of Chinese national digital television terrestrial broadcasting standard [2] and its performance has been extensively tested and verified [3], simply because spectral efficiency is one of the major concerns for wireless systems.

Until now, TDS-OFDM has only been used in the downlink broadcasting. If TDS-OFDM were to be extended to uplink multiple access application, it would be very difficult to eliminate the superimposed multi-user interference using the

conventional iterative methods (see [1] and the references therein), since the user-specific ISI has to be removed one by one. This technical difficulty has prevented the extension of the single-user TDS-OFDM to multi-user scenarios.

CP based orthogonal frequency division multiple access (CP-OFDMA) has been widely adopted as a multiple access solution in many wireless communication standards, such as the uplink of the interaction channel for digital terrestrial television (DVB-RCT) [4], IEEE 802.16e standard for mobile broadband wireless access systems (WiMax) [5], and the next generation of broadband wireless networks [6]. This letter proposes an alternative uplink multiple access solution, referred to as the TDS frequency division multiple access (TDS-FDMA), by extending the single-user TDS-OFDM concept. The main contributions of this letter are summarised as below.

- 1) The specially designed frame structure makes the CE and IC completely separated from each other. Therefore, the joint cyclicity reconstruction of the received IDFT block for all the users is simply achieved by a one-step add-subtraction operation without the need of CE information. Moreover, the preamble in the frame structure enables accurate joint CE for all active users based on a one-step circular correlation.
- 2) Compared with standard CP-OFDMA systems, the proposed TDS-FDMA improves the spectral efficiency by about 5% to 10% as well as achieves slightly better bit error rate (BER) performance, while practically imposing a similarly low computational complexity. In addition, the proposed TDS-FDMA system provides a unified transceiver architecture for both the single-carrier (SC) and multi-carrier (MC) uplink multiple access.

Throughout this contribution, upper- and lower-case letters represent the FD and time-domain (TD) symbols, respectively, while boldfaced letters denote matrices or column vectors. However, for notational convenience, the notation of a sequence is interchangeable to a column vector.  $\mathbf{I}_N$  is the  $N \times N$  identity matrix and  $\star$  denotes the linear convolution, while  $\otimes$  represents the circular correlation.  $(\cdot)^*$ ,  $(\cdot)^T$  and  $(\cdot)^H$  represent the complex conjugate, transpose and conjugate transpose operators, respectively, while  $(\cdot)]_N$  is the modulo- $N$  operation. Furthermore,  $E\{\cdot\}$  and  $\text{tr}\{\cdot\}$  are the expectation and trace operators, respectively, while  $\hat{x}$  denotes an estimate of  $x$  and  $\delta(n)$  is the Kronecker delta function.

The rest of this letter is organized as follows. Section II describes the proposed TDS-FDMA transmission scheme, while the TDS-FDMA receiver design is detailed in Section III. Section IV compares the performance of the proposed TDS-FDMA system with that of the standard CP-OFDMA, and conclusions are drawn in Section V.

Manuscript received June 30, 2010; revised December 7, 2010; accepted December 16, 2010. The associate editor coordinating the review of this letter and approving it for publication was C. Xiao.

L. Dai and Z. Wang are with the Department of Electronic Engineering, Tsinghua University, Beijing 100084, China (e-mail: dll07@mails.tsinghua.edu.cn, zcwang@mail.tsinghua.edu.cn).

S. Chen is with the School of Electronics and Computer Science, University of Southampton, Southampton SO17 1BJ, UK (e-mail: sq@ecs.soton.ac.uk).

This work was supported in part by Standardization Administration of the People's Republic of China with AQSIQ Project 200910244 and in part by Tsinghua University Initiative Scientific Research Program 20091081280. Part of this work was presented at 2010 IEEE GLOBECOM.

Digital Object Identifier 10.1109/TWC.2011.01111.102070

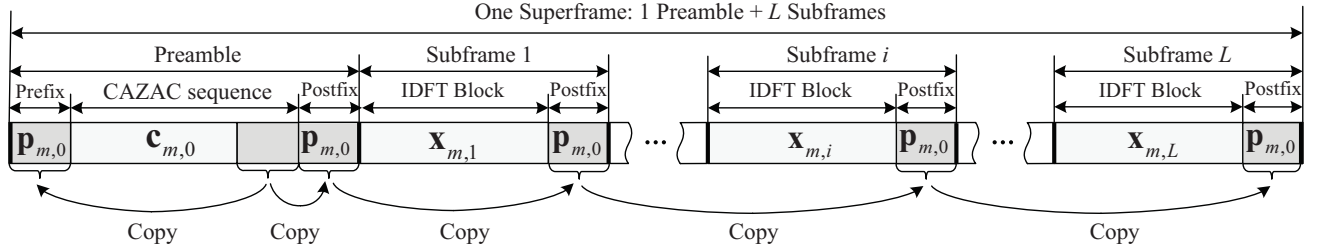


Fig. 1. Transmission frame structure of the TDS-FDMA system.

## II. PROPOSED TDS-FDMA TRANSMISSION SCHEME

Figure 1 shows the frame structure for the  $m$ th user of the proposed TDS-FDMA system with  $M$  active users, in which every user adopts this identical frame structure. The block transmission unit is the superframe, which consists of one preamble and  $L$  subframes. The subframe is equivalent to one OFDM symbol, and the number of subframes  $L$  can be flexibly designed according to the channel's coherent time, i.e., a higher Doppler spread leads to a smaller  $L$  and vice versa [7]. The  $N_g$ -point preamble in the superframe consists of three parts: the user-specific  $N_p$ -point training sequence  $\mathbf{c}_{m,0} = \{c_{m,0}(n)\}_{n=0}^{N_p-1}$ , the  $K$ -point prefix and the  $K$ -point postfix, which are identical and can be denoted as  $\mathbf{p}_{m,0} = \{p_{m,0}(n)\}_{n=0}^{K-1}$ . Instead of using a PN sequence with good but non-ideal autocorrelation as adopted in the TDS-OFDM system, a constant amplitude zero autocorrelation (CAZAC) sequence with perfect autocorrelation and flat frequency response is used as the training sequence for the proposed TDS-FDMA scheme. According to [8], the CAZAC sequence  $\mathbf{c}_{m,0}$  can be chosen as

$$c_{m,0}(n) = e^{j\frac{\pi r n^2}{N_p}}, \quad 0 \leq n \leq N_p - 1, \quad 1 \leq m \leq M, \quad (1)$$

where  $r$  is relatively prime to  $N_p$ . The autocorrelation of the CAZAC sequence (1) is given by

$$R_c(k) = \sum_{n=0}^{N_p-1} c_{m,0}^*(n) c_{m,0}((n+k) \bmod N_p) = \begin{cases} N_p, & k=0, \\ 0, & k \neq 0. \end{cases} \quad (2)$$

Unlike the frame header of the TDS-OFDM system where cyclic prefix and cyclic postfix with different lengths and distinct contents are used [2], the prefix and the postfix in the TDS-FDMA system are exactly the same, both of which are the last  $K$  symbols of the CAZAC sequence  $\mathbf{c}_{m,0}$ . Therefore,  $N_g = N_p + 2K$ . For supporting multiple users, the user-specific CAZAC sequences between neighbouring users hold a constant circular shift  $N_s$ , which can be represented by

$$\mathbf{c}_{m,0} = \mathbf{c}_{m',0}^{\oplus(m-m')N_s}, \quad 1 \leq m, m' \leq M, \quad (3)$$

where  $\mathbf{c}_{m,0}$  and  $\mathbf{c}_{m',0}$  are the CAZAC sequences for the  $m$ th and  $m'$ th users, respectively, while  $\mathbf{c}^{\oplus N_s}$  denotes the  $N_s$ -symbol circular shift of  $\mathbf{c}$ . The CAZAC training sequence design with TD circular shift is to facilitate the joint CE at the receiver, which will be addressed in Subsection III-B.

The  $i$ th  $N_f$ -point subframe  $\mathbf{s}_{m,i} = \{s_{m,i}(n)\}_{n=0}^{N_f-1} = \{\mathbf{x}_{m,i}, \mathbf{p}_{m,i}\}$  within the superframe is the serial concatenation of the  $N$ -point IDFT data block  $\mathbf{x}_{m,i} = \{x_{m,i}(n)\}_{n=0}^{N-1}$ , whose discrete Fourier transform (DFT) is represented by  $\mathbf{X}_{m,i} = \{X_{m,i}(k)\}_{k=0}^{N-1}$ , and the  $K$ -point postfix  $\mathbf{p}_{m,i} =$

$\{p_{m,i}(n)\}_{n=0}^{K-1}$ , where  $N_f = N + K$ . The postfix  $\mathbf{p}_{m,i}$  in each subframe is not related to the IDFT block  $\mathbf{x}_{m,i}$ , but is identical to the prefix and postfix in the preamble, that is,  $\mathbf{p}_{m,i} = \mathbf{p}_{m,0}$  for  $1 \leq i \leq L$ . The identical postfixes ensure the low-complexity joint cyclicity reconstruction of the received IDFT block, which will be discussed in Subsection III-A.

The IDFT block  $\mathbf{x}_{m,i}$  can be either a MC OFDMA signal [9] or a SC FDMA signal [10]. In both cases,  $\mathbf{X}_{m,i}$ ,  $1 \leq m \leq M$ , are mutual orthogonal among different users. Without the loss of generality, an OFDMA type signal is assumed in the sequel.

## III. PROPOSED TDS-FDMA RECEIVER DESIGN

### A. Joint Cyclicity Reconstruction

Let the channel impulse response (CIR) for the  $m$ th user be denoted by  $\mathbf{h}_{m,i} = \{h_{m,i}(l)\}_{l=0}^{l_{m,i}-1}$  for  $0 \leq i \leq L$ , where  $l_{m,i}$  represents the maximum channel delay spread of  $\mathbf{h}_{m,i}$ ,  $\mathbf{h}_{m,0}$  is the CIR for the preamble, while  $\mathbf{h}_{m,i}$ ,  $1 \leq i \leq L$ , is the CIR for the  $i$ th subframe. Let  $l_{\max} = \max\{l_{m,i}, 1 \leq m \leq M, 0 \leq i \leq L\}$ , and  $l_{\max} \leq K + 1$  is assumed. We denote the  $(N+K)$ -length signal  $\mathbf{y}_i = \{y_i(n)\}_{n=0}^{N+K-1}$  as the convolution of the transmitted  $N$ -length IDFT blocks  $\{\mathbf{x}_{m,i}\}_{m=1}^M$  with the multi-path channels as below

$$y_i(n) = \sum_{m=1}^M y_{m,i}(n) = \sum_{m=1}^M (x_{m,i}(n) \star h'_{m,i}(n) + v_{m,i}(n)), \quad (4)$$

where  $\mathbf{h}'_{m,i}$  is the  $(K+1)$ -dimensional vector generated by padding zeros to the end of  $\mathbf{h}_{m,i}$ , and  $v_{m,i}(n)$  the additive white Gaussian noise (AWGN) sample. The cyclicity reconstruction of the received IDFT block is essential to convert the linear convolution between  $\mathbf{x}_{m,i}$  and  $\mathbf{h}'_{m,i}$  into a circular convolution for a low-complexity FD equalization (FDE).

Let  $\{r_{m,i}(n)\}_{n=0}^{N-1}$  be the actually received IDFT block in the  $i$ th subframe,  $\{r_{m,i}(n+N)\}_{n=0}^{K-1}$  the received postfix in the  $i$ th subframe, and  $\{r_{m,0}(n+N_p+K)\}_{n=0}^{K-1}$  the received postfix in the preamble for the  $m$ th user. The following one-step add-subtraction operation between the received IDFT block, the postfix in the subframe and the postfix in the preamble will produce the jointly cyclicity reconstructed  $N$ -point signal  $\mathbf{y}'_i = \{y'_i(n)\}_{n=0}^{N-1}$  of the received IDFT block

$$y'_i(n) = \begin{cases} \sum_{m=1}^M (r_{m,i}(n) + r_{m,i}(n+N) - r_{m,0}(n+N_p+K)), & 0 \leq n \leq K-1, \\ \sum_{m=1}^M r_{m,i}(n), & K \leq n \leq N-1. \end{cases} \quad (5)$$

Assume that the channel is quasi-static within one superframe. Then  $\mathbf{h}_{m,i} = \mathbf{h}_{m,0}$  for  $1 \leq i \leq L$ , and the postfix in the

preamble and the postfix in the  $i$ th subframe will introduce the same ‘tail’ due to the multi-path dispersion, yielding

$$y'_i(n) = \sum_{m=1}^M y'_{m,i}(n), \quad 0 \leq n \leq N-1, \quad (6)$$

where

$$y'_{m,i}(n) = \begin{cases} y_{m,i}(n+N) + y_{m,i}(n), & 0 \leq n \leq K-1, \\ y_{m,i}(n), & K \leq n \leq N-1. \end{cases} \quad (7)$$

Clearly,  $y'_{m,i}$  in (7) takes the exactly same form as that of a received IDFT block after removing the CP in the single-user CP based OFDM system. Consequently,  $y'_i$  in (6), which is a linear combination of  $\{y'_{m,i}\}_{m=1}^M$ , holds the cyclicity property. Thus, the joint cyclicity reconstruction for all the users is achieved via the one-step add-subtraction operation (5). Note that this one-step add-subtraction operation only introduces very marginally more computation than simply removing the CP in a CP-OFDMA system, and the proposed TDS-FDMA practically imposes a similarly low computational complexity as a standard CP-OFDMA system does.

The noise in the received signal has a direct impact on the cyclicity reconstruction process, and the signal-to-noise ratio (SNR) loss due to the add-subtraction operation is

$$\text{SNR}_{\text{loss}} = 10 \cdot \log_{10} \left( \frac{2K+N}{N} \right). \quad (8)$$

Unlike the conventional TDS-OFDM where CE and cyclicity reconstruction are coupled, the proposed joint cyclicity reconstruction via the add-subtraction operation (5) requires no channel information, and thus CE errors have no impact on the performance of cyclicity reconstruction. Moreover, the proposed scheme does not suffer from the severe SNR loss caused by the iterative CE and IC process of the conventional scheme. It should also be pointed out that the above cyclicity reconstruction method still works for time-varying channels, and this will be confirmed in the simulation study.

After the cyclicity reconstruction, the  $N$ -point DFT of  $y'_i$  yields the FD received IDFT block  $Y'_i = \{Y'_i(k)\}_{k=0}^{N-1}$  with the entries

$$Y'_i(k) = \sum_{m=1}^M X_{m,i}(k) H_{m,i}(k) + V_i(k), \quad (9)$$

where  $H_{m,i}$  is the DFT of  $\mathbf{h}_{m,i}$ , and  $V_i(k)$  denotes the AWGN with  $E\{|V_i(k)|^2\} = \sigma^2$ . Since the multi-users' data  $\{\mathbf{X}_{m,i}\}_{m=1}^M$  are mutual orthogonal in the FD, zero-forcing (ZF) or alternatively the minimum mean square error (MMSE) FDE can be used to restore the user-specific transmitted signals  $\{\mathbf{X}_{m,i}\}_{m=1}^M$  if  $\{\mathbf{H}_{m,i}\}_{m=1}^M$  or  $\{\mathbf{h}_{m,i}\}_{m=1}^M$  is known, which is the topic of the following subsection.

### B. Joint Channel Estimation

Assuming that  $l_{\max} \leq N_s$  and  $M \cdot N_s = N_p$ , the actually received CAZAC sequence protected by the prefix in the preamble can be expressed as

$$\mathbf{g}_0 = \sum_{m=1}^M \tilde{\mathbf{C}}_{m,0} \vec{\mathbf{h}}_{m,0} + \mathbf{w}_0 = \mathbf{C}_0 \mathbf{h}_{\text{total}} + \mathbf{w}_0, \quad (10)$$

where  $\tilde{\mathbf{C}}_{m,0}$  is the  $N_p \times N_s$  circular matrix whose first column is the CAZAC vector  $\mathbf{c}_{m,0}$ ,  $\vec{\mathbf{h}}_{m,0}$  is the  $N_s \times 1$  vector obtained by padding zeros to the end of the original CIR vector  $\mathbf{h}_{m,0}$ ,  $\mathbf{C}_0 = [\tilde{\mathbf{C}}_{1,0} \ \tilde{\mathbf{C}}_{2,0} \ \cdots \ \tilde{\mathbf{C}}_{M,0}]$  is the  $N_p \times N_p$  training sequence matrix,  $\mathbf{h}_{\text{total}} = [\vec{\mathbf{h}}_{1,0}^T \ \vec{\mathbf{h}}_{2,0}^T \ \cdots \ \vec{\mathbf{h}}_{M,0}^T]^T$  is the  $N_p \times 1$  total channel vector,  $\mathbf{w}_0$  denotes the AWGN vector with  $E\{\mathbf{w}_0 \mathbf{w}_0^H\} = \sigma^2 \mathbf{I}_{N_p}$ . The least squares (LS) estimation of the channel vector  $\mathbf{h}_{\text{total}}$  in (10) is given by [11]

$$\hat{\mathbf{h}}_{\text{total}} = (\mathbf{C}_0^H \mathbf{C}_0)^{-1} \mathbf{C}_0^H \mathbf{g}_0. \quad (11)$$

The mean square error (MSE) of the LS channel estimation (LSCE) (11) is defined by

$$\begin{aligned} \text{MSE} &= E \left\{ \text{tr} \left\{ \left( \hat{\mathbf{h}}_{\text{total}} - \mathbf{h}_{\text{total}} \right)^H \left( \hat{\mathbf{h}}_{\text{total}} - \mathbf{h}_{\text{total}} \right) \right\} \right\} \\ &= E \left\{ \text{tr} \left\{ \left( \mathbf{C}_0^H \mathbf{C}_0 \right)^{-1} \mathbf{C}_0^H \mathbf{w}_0 \mathbf{w}_0^H \mathbf{C}_0 \left( \mathbf{C}_0^H \mathbf{C}_0 \right)^{-1} \right\} \right\} \\ &= \sigma^2 \text{tr} \left\{ \left( \mathbf{C}_0^H \mathbf{C}_0 \right)^{-1} \right\}. \end{aligned} \quad (12)$$

The MMSE of the LSCE is achieved if and only if

$$\mathbf{C}_0^H \mathbf{C}_0 = N_p \mathbf{I}_{N_p}. \quad (13)$$

In this case, the LSCE (11) is simplified to

$$\hat{\mathbf{h}}_{\text{total}} = \frac{1}{N_p} \mathbf{C}_0^H \mathbf{g}_0 = \mathbf{h}_{\text{total}} + \frac{1}{N_p} \mathbf{C}_0^H \mathbf{w}_0, \quad (14)$$

and the corresponding MMSE can be derived from (12) as

$$\text{MSE}_{\min} = \sigma^2. \quad (15)$$

Clearly, the CAZAC sequences with the ideal autocorrelations given in (2) and the circular shifted structure defined by (3) lead to the training sequence matrix  $\mathbf{C}_0$  that meets (13). Thus a reliable CE, which attains the MMSE accuracy (15), can be achieved for the TDS-FDMA system. Owing to the circular property of the CAZAC training sequence matrix  $\mathbf{C}_0$ , the unbiased LSCE (14) can also be expressed in the form of circular correlation as follows

$$\begin{aligned} \hat{\mathbf{h}}_{\text{total}} &= \frac{1}{N_p} \mathbf{c}_{0,0}^* \otimes \mathbf{g}_0 = \frac{1}{N_p} \mathbf{c}_{0,0}^* \otimes \left( \sum_{m=1}^M \mathbf{c}_{m,0} \otimes \mathbf{h}_{m,0} + \mathbf{w}_0 \right) \\ &= \sum_{m=1}^M \mathbf{h}_{m,0} \delta(n - (m-1)N_s) + \frac{1}{N_p} \mathbf{c}_{0,0}^* \otimes \mathbf{w}_0. \end{aligned} \quad (16)$$

The user-specific CIR estimate  $\hat{\mathbf{h}}_{m,0}$  can be directly selected from  $\hat{\mathbf{h}}_{\text{total}}$ . When the channel is slowly time-varying,  $\hat{\mathbf{h}}_{m,i} = \hat{\mathbf{h}}_{m,0}$  for  $1 \leq i \leq L$  can be assumed to equalize the  $L$  subframes following the preamble. However, if the channel is varying fast, this mechanism will lead to inaccurate estimates  $\hat{\mathbf{h}}_{m,i}$  and consequently poor channel equalization performance, particularly for those subframes located near the end of a superframe. The following low-complexity linear interpolation can be used to reduce the CE error

$$\hat{\mathbf{h}}_{\text{total},i}^{\{j\}} = \frac{i-1}{L-1} \left( \hat{\mathbf{h}}_{\text{total}}^{\{j+1\}} - \hat{\mathbf{h}}_{\text{total}}^{\{j\}} \right) + \hat{\mathbf{h}}_{\text{total}}^{\{j\}}, \quad 1 \leq i \leq L, \quad (17)$$

where  $\hat{\mathbf{h}}_{\text{total}}^{\{j\}}$  denotes the preamble based LSCE (16) for the  $j$ th superframe,  $\hat{\mathbf{h}}_{\text{total},i}^{\{j\}}$  is the interpolated total CIR estimate

TABLE I  
SPECTRAL EFFICIENCY COMPARISON BETWEEN DVB-RCT AND  
TDS-FDMA IN TERMS OF PERCENTAGE WITH RESPECT TO  $\eta_0$

Guard interval length	DVB-RCT with BS1	DVB-RCT with BS2	DVB-RCT with BS3	TDS-FDMA
$K = N/8$	71.11%	72.73%	73.56%	78.43%
$K = N/16$	75.29%	77.00%	77.89%	84.21%
$K = N/32$	77.58%	79.34%	80.25%	87.80%

TABLE II  
TDS-FDMA SYSTEM PARAMETERS FOR SIMULATION

Central carrier frequency	770 MHz
Signal bandwidth	7.56 MHz
IDFT block signal type	OFDMA
Carrier allocation scheme	Generalized
Number of active users $M$	4
Total sub-carriers $N$	3780
Symbol rate	7.56 MHz
Sub-carrier spacing	2 kHz
Modulation schemes	16QAM/64QAM
Training sequence length $N_p$	255
Postfix length $K$	64
Subframe number $L$	5
Maximum Doppler spread $f_d$	5/20/50 Hz

for the  $i$ th subframe of the  $j$ th superframe. More sophisticated signal processing techniques, such as Kalman filter or higher order interpolation [12], can also be used for more accurate channel tracking.

Note that the preamble based CE can be used for both SC and MC transmissions in TDS-FDMA. In addition, the identical postfixes provide the cyclic property in the frame structure, which can be used for uplink timing and carrier frequency offset synchronization [13]. The correlation peaks obtained in (16) also provide additional alternatives for synchronization.

### C. Spectral Efficiency

For typical CP-OFDMA schemes such as the DVB-RCT standard [4], both FD pilots and TD CP insertions result in a loss in spectral efficiency [14]. The spectral efficiency of the DVB-RCT system is calculated as

$$SE_{\text{DVB-RCT}} = \eta_0 \times \frac{N_d}{N_d + N_c} \times \frac{N}{N + K}, \quad (18)$$

where  $\eta_0$  [bit/s/Hz] is the spectral efficiency of an ideal OFDM-type system without pilots and guard interval,  $K$  is the CP length, while  $N_d$  and  $N_c$  are the numbers of the user data symbols and pilot symbols in the DVB-RCT burst structure (BS). Specifically, DVB-RCT specifies three types of BS, referred to as BS1, BS2 and BS3, where  $N_d = 144$  is adopted for all the three BSs, while  $N_c = 36$  for BS1,  $N_c = 32$  for BS2 and  $N_c = 30$  for BS3, respectively.

The spectral efficiency of the proposed TDS-FDMA system is given by

$$SE_{\text{TDS-FDMA}} = \eta_0 \times \frac{LN}{L(N + K) + N_p + 2K}. \quad (19)$$

Note that a larger sequence length  $N_p$  provides better CE and supports higher number of users, but results in the reduced spectral efficiency for the TDS-FDMA.

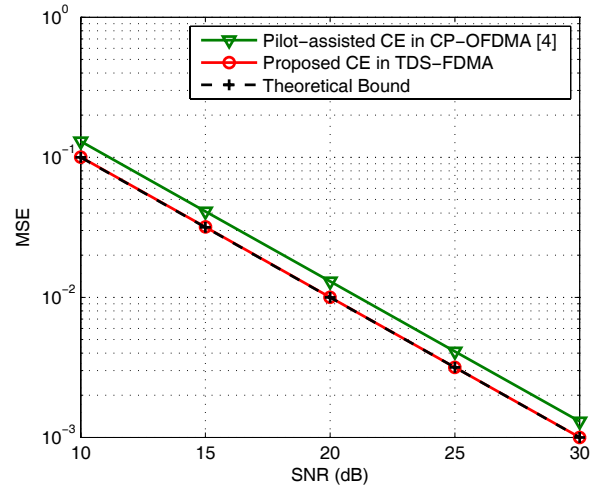


Fig. 2. Channel estimation performance comparison of the proposed TDS-OFDM and standard CP-OFDMA systems over the Vehicular-A channel.

Obviously, spectral efficiency can also be expressed in percentage if  $\eta_0$  is taken as the reference. Because the DVB-RCT system can update the channel state information every 6 OFDMA signal frames with the pilot insertion scheme [4], we select  $L = 5$  and set the length of the CAZAC sequence to  $N_p = 1024$  for the TDS-FDMA system to ensure a fair comparison. Table I compares the spectral efficiency of the proposed TDS-FDMA system with that of the DVB-RCT in the 2K mode ( $N = 2048$  for both the DVB-RCT and TDS-FDMA), where it can be seen that the TDS-FDMA system improves the spectral efficiency by about 5% to 10%, in comparison with the DVB-RCT system. This clearly demonstrates that the TDS-FDMA system achieves a better spectral efficiency than typical OFDMA systems such as the DVB-RCT.

## IV. SIMULATION RESULTS

The TDS-FDMA system parameters used in the simulation are listed in Table II. The DVB-RCT using BS3 [4] was also simulated as a typical CP-OFDMA system, with the system's parameters set to the compatible values to those of the TDS-FDMA system.

Figure 2 compares the MSE performance of the CE for the proposed TDS-FDMA system with that of the simulated CP-OFDMA system over the Vehicular-A channel [15]. Compared with the pilot-assisted CE in CP-OFDMA systems, the preamble based CE in the TDS-FDMA system achieves an SNR improvement of about 1.0 dB at the MSE level of  $10^{-2}$ . This is because the TD LSCE method of the TDS-FDMA system directly obtains the complete CIR estimate, while the pilot-aided FD CE in the CP-OFDMA can only acquire the channel frequency response (CFR) estimate at the pilot subcarriers, and the estimated CFR may not be accurate over the deeply fading subcarriers. Moreover, it is seen from Fig. 2 that the simulated MSE performance of the proposed CE attains the theoretical MMSE bound given in (15).

Figs. 3 and 4 show the averaged BER performance comparison of the proposed TDS-FDMA and simulated CP-OFDMA systems over the Vehicular-A Rayleigh fading channel for the 16QAM and 64QAM modulation schemes, respectively.

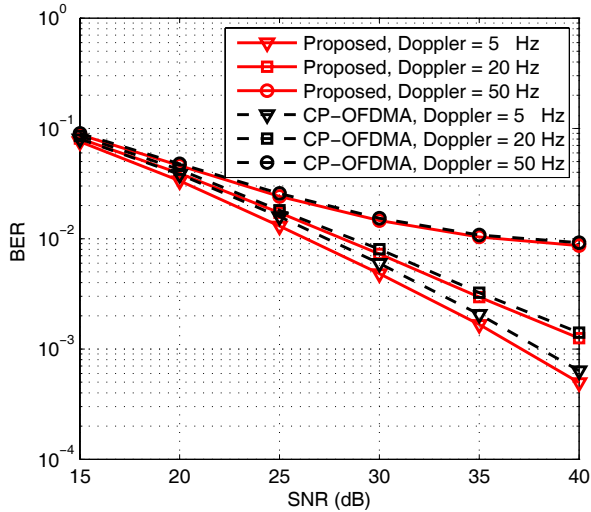


Fig. 3. BER performance comparison of the proposed TDS-FDMA and standard CP-OFDMA systems over the Vehicular-A Rayleigh fading channel with the 16QAM modulation.

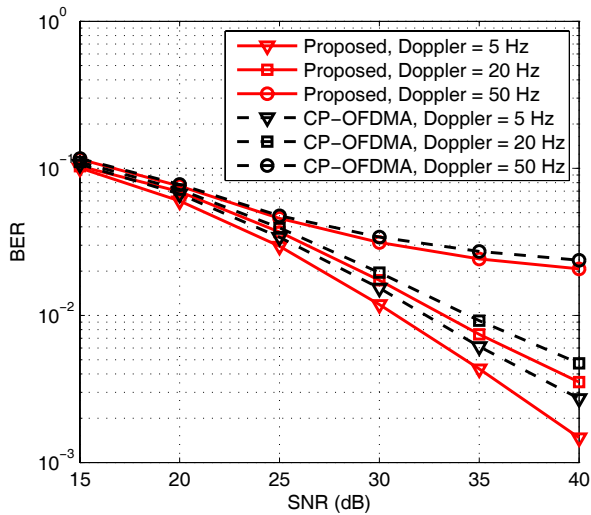


Fig. 4. BER performance comparison of the proposed TDS-FDMA and standard CP-OFDMA systems over the Vehicular-A Rayleigh fading channel with the 64QAM modulation.

The ZF FDE was used for the both systems. For the 16QAM scheme, the TDS-FDMA achieves an SNR gain of about 0.8 dB over the simulated CP-OFDMA at the BER level of  $10^{-2}$  when  $f_d = 5$  Hz, while the SNR gain is about 0.3 dB when  $f_d = 20$  Hz. For the 64QAM scheme, the achieved SNR gains of the proposed TDS-FDMA over the standard CP-OFDMA at the BER level of  $10^{-2}$  are 1.5 dB and 1.0 dB, respectively, when  $f_d = 5$  Hz and 20 Hz. For the high Doppler spread of  $f_d = 50$  Hz, the SNR gain of the TDS-FDMA over the simulated CP-OFDMA becomes marginal and negligible, as can be seen from Figs. 3 and 4. Performance of the TDS-FDMA at high Doppler spread may be improved by either decreasing the subframe number  $L$  or employing other signal processing techniques such as blind equalization [16].

## V. CONCLUSIONS

A novel uplink multiple access scheme called the TDS-FDMA has been proposed to support multi-user uplink application. The specially designed frame structure enables the low-complexity implementation of joint cyclicity reconstruction and channel estimation at the receiver. Compared with standard CP-OFDMA systems, the proposed TDS-FDMA scheme achieves a higher spectral efficiency and slightly better BER performance, while only imposing a very marginally higher complexity. The proposed TDS-FDMA also supports both multi-carrier and single-carrier transmissions, which makes it a promising candidate for the wireless interactive return channel solution for Chinese future digital television standard. Our future study includes the optimal receiver design for the proposed transmission scheme to explore additional benefits [17], and the hybrid design of TDS-FDMA and TDMA to support more flexible multiple access.

## REFERENCES

- [1] J. Wang, Z. Yang, C. Pan, and J. Song, "Iterative padding subtraction of the PN sequence for the TDS-OFDM over broadcast channels," *IEEE Trans. Consumer Electron.*, vol. 51, no. 11, pp. 1148-1152, Nov. 2005.
- [2] Framing Structure, Channel Coding and Modulation for Digital Television Terrestrial Broadcasting System, Chinese National Standard, GB 20600-2006, Aug. 2006.
- [3] C. yen Ong, J. Song, C. Pan, and Y. Li, "Technology and standards of digital television terrestrial multimedia broadcasting," *IEEE Commun. Mag.*, vol. 48, no. 5, pp. 119-127, May 2010.
- [4] Digital Video Broadcasting (DVB); Interaction Channel for Digital Terrestrial Television (RCT) Incorporating Multiple Access OFDM, ETSI, EN 301 958, Mar. 2002.
- [5] IEEE Standard for Local and Metropolitan Area Networks—Part 16: Air Interface for Fixed and Mobile Broadband Wireless Access Systems, IEEE 802.16e, Feb. 2006.
- [6] H. Chen, X. Zhang, and W. Xu, "Next-generation CDMA vs. OFDMA for 4G wireless applications," *IEEE Trans. Wireless Commun.*, vol. 14, no. 3, pp. 6-7, June 2007.
- [7] L. Dai, Z. Wang, J. Wang, and Z. Yang, "A novel TDS-FDMA scheme for multi-user uplink scenarios," in *Proc. IEEE GLOBECOM '2010*, Dec. 2010.
- [8] L. Boemer and M. Antweiler, "Perfect N-phase sequences and arrays," *IEEE J. Sel. Areas Commun.*, vol. 10, no. 4, pp. 782-789, May 1992.
- [9] H. Li and H. Liu, "An analysis of uplink OFDMA optimality," *IEEE Trans. Wireless Commun.*, vol. 6, no. 8, pp. 2972-2983, Aug. 2007.
- [10] O. Oteri, I. Wong, and W. McCoy, "Optimal resource allocation in uplink SC-FDMA systems," *IEEE Trans. Wireless Commun.*, vol. 8, no. 5, pp. 2161-2165, May 2009.
- [11] S. M. Kay, *Fundamentals of Statistical Signal Processing, Volume I: Estimation Theory*. Prentice-Hall, 1993.
- [12] B. Karakaya, H. Arslanand, and H. A. Cirpan, "An adaptive channel interpolator based on Kalman filter for LTE uplink in high Doppler spread environments," *EURASIP J. Wireless Commun. Netw.*, vol. 2009, no. 7, pp. 1-10, Mar. 2009.
- [13] M. Morelli, C.-C. J. Kuo, and M.-O. Pun, "Synchronization techniques for orthogonal frequency division multiple access (OFDMA): a tutorial review," *Proc. IEEE*, vol. 95, no. 7, pp. 1394-1427, July 2007.
- [14] X. Wang, Y. Wu, J.-Y. Chouinard, and H.-C. Wu, "On the design and performance analysis of multisymbol encapsulated OFDM systems," *IEEE Trans. Veh. Technol.*, vol. 55, no. 3, pp. 990-1002, May 2006.
- [15] Guideline for Evaluation of Radio Transmission Technology for IMT-2000, Recommendation ITU-R M.1225, 1997.
- [16] S. Chen, W. Yao, and L. Hanzo, "Semi-blind adaptive spatial equalization for MIMO systems with high-order QAM signalling," *IEEE Trans. Wireless Commun.*, vol. 7, no. 11, pp. 4486-4491, Nov. 2008.
- [17] S. Zhou and G. B. Giannakis, "Single-carrier space-time block-coded transmissions over frequency-selective fading channels," *IEEE Trans. Inf. Theory*, vol. 49, no. 1, pp. 164-178, Jan. 2003.